Lysozyme Partitioning in Novel Aqueous-two Phase Systems based on Hyperbranched Polymers

Beatriz Fernandes
Instituto Superior Técnico, Lisboa, Portugal

September 2015

Abstract

Aqueous two-phase systems (ATPS) constitute a promising process technology for the separation and purification of biomolecules. Despite scalability and mild extraction conditions, commercial application is scarce due to multiplicity of process variables, which lead to significant experimental efforts towards the design of ATPS processes. The aim of this work is to study and model the partitioning of lysozyme in ATPSs with linear and hyperbranched polymers (HBP) as phase forming components. Dextran T40 and polyethylene glycol (PEG) polymers with a molar mass of 6000 and 8000 were chosen as linear polymers. The used HBP were hyperbranched polyester with a PEG core and 2,2-bis(methylol)propionic acid branching units. The Lattice Cluster Theory (LCT) in combination with the Wertheim Association Theory was used to model the studied ATPSs and the lysozyme partitioning. The goal was partially achieved as the partitioning in the HBPs based ATPS could not be measured. Although, the ternary systems polymer – polymer – water were successfully modelled as well as the lysozyme partitioning coefficients in the linear polymers' based systems.
Keywords: Aqueous Two-Phase Systems (ATPS), Lysozyme, Lattice Cluster Theory (LCT), Whertheim Theory, Partition.

ATPS Aqueous Two Phase Systems
bis-MPA 2,2-bis(methylol)propionic acid
EOS Equation of State
FH Flory-Huggins
G2 PFLDHB-G2-PEG6k-OH
G3 PFLDHB-G3-PEG6k-OH
HBP Hyperbranched Polymers
HPLC High-performance Liquid Chromatography
LCT Lattice Cluster Theory
LLE Liquid-Liquid Equilibrium
NRTL Non Random Two Liquids
PEG Polyethylene Glycol
SAFT Statistical Association Fluid Theory
TLL Tie Line Length
UNIQUAC Universal Quasichemical

1. Introduction

Over the last 20 years a great productivity increase took place in the biomanufacturing industry. Titers of recombinant proteins in fermentation broths were boosted from a scale of milligrams to grams per litre [1]. This development was especially motivated by the increasing market value of biopharmaceutical products, particularly antibodies and proteins [2]. Simultaneously, downstream processing did not keep up with the productivity improvement, despite still being the main responsible for the production cost of biopharmaceuticals (between 45% and 92% [3]), thus creating a bottleneck in the biotechnological industry [4].

Notably, therapeutic proteins require high purification values (<0,1% impurities [5]). Proteins derive their functions from a complex three-dimensional structure that can easily be lost when subjected to pH and temperature values far from moderate. Moreover, structural damage can be irreversible, leading to biomolecules without functionality, and therefore, value. Chromatography is a simple process with a high resolving power that embodies the right conditions for the purification of biomolecules. For that reason it becomes indispensable as a unit operation. However, it has low capacity and is difficult to scale up, hence being one of the reasons for the high costs of downstream processing [6]. In an attempt to either replace chromatography or reduce the load of impurities in the feedstream so that one or more chromatography stages can be eliminated, alternative separation processes have been proposed. Aqueous Two Phase Systems (ATPS) show potential to overcome the limitations of chromatography.

ATPS are formed by mixing two hydrophilic, incompatible components, such as a salt and a polymer, a salt and an alcohol, two hydrophilic polymers or two surfactants in water above a critical concentration [7]. These systems can be used effectively for the separation and purification of proteins given

that both phases consist mainly of water, and have a low interfacial tension resulting in a low mechanical stress on the proteins during the extraction process. The practical application of ATPS has been demonstrated on a large number of cases with excellent levels of purity and yield [8].

In an attempt to describe the phase equilibria in ATPS, different models were developed, which can be segregated based on divergent schools of thought. The first modelling approaches were based on the Othmer-Tobias [9] and Bancroft [10] equations, which required an input of experimental data and several adjusted parameters to model the tie-lines. Other models are based on osmotic viral expansions, reminiscent of the work of Edmond and Ogston [11][12]. These do not require experimental data input, but involve up to three adjustable parameters to describe the interaction between the different components, and an extra one to account for the temperature influence. Besides the correlation equations, thermodynamic models using Equation of State (EOS) and the Gibbs excess energy (G^E) equations where also introduced to perform calculations in order to characterize the ATPS. One possible way is the use of EOS, such as Statistical Association Fluid Theory (SAFT)-family equations, which originated from a perturbation theory inspired by Wertheim papers [13]. The EOS models are useful when modelling different phase diagrams with polymers present in the mixture, and normally pure component data are used to fit the model parameter of an EOS as density or vapour pressure, but depend upon high calculation efforts and the parameters of pure components must be fitted to phase equilibria data. The G^E models have also been applied to calculate the phase behaviour of ATPS. These models can take into account short range interactions, such as the Non Random Two Liquids (NRTL), extended NRTL, Wilson or Universal Quasichemical (UNIQUAC) models, or long range interactions, in the case of Debye-Hueckle and Pitzer-Debye-Hueckle [14]. The drawback of the G^E models is the lack of associative interactions which are of great importance for the thermochemical modelling of liquid systems.

Lastly, there are also models based on extensions of lattice theories (also G^E models) such as the Flory-Huggins (FH) theory [15] [16], which is the classical way of describing phase behaviour in polymer solutions. However this theory is a simple mean-field approximation that ignores the details of the polymer structure, and therefore, is not suitable for non-linear polymers. The Lattice Cluster Theory (LCT) is an extension of the FH theory, developed by Freed and co-workers [17, 18, 19, 20, 21], that takes into account polymer structure.

Kulaguin Chicaroux and Zeiner [22] published a G^E model based on the LCT to calculate the ATPS taking into account on the one hand the molecular structure, derived from the LCT, and on the other hand the associative interactions by integrating the Wertheim association theory [23, 24].

2. Experimental

2.1. Materials

In this study Polyethylene Glycol (PEG) 6000, PEG 8000 and dextran were used as the linear polymers to form the ATPS, while PFLDHB-G2-PEG6k-OH (G2) and PFLDHB-G3-PEG6k-OH (G3) were applied as the branched polymers (Table 1). All the chemicals were used without further purification. With the help of weak heating and magnetic stirring, all polymers can be dissolved in water quickly.

The linear PEG polymers share the chemical formula $HO(C_2H_4O)_nH$. PEG 6000, from Merck Schuchardt OHG, Hohenbrunncan, Germany, can be characterized as a white or almost white solid with a waxy or paraffin-like appearance. PEG 8000 is a white waxy powder from AMRESCO, 6681 Cochran Rd, United States. The chemical formula of dextran is $(C_6H_{10}O_5)_n$ and at room temperature it is a white power. It is produced by Carl Roth GmbH + Co. KG, Karlsruhe. All the mentioned polymers were stored at room temperature in a closed container opened only for experiments.

The Hyperbranched Polymers (HBP) both have the appearance of a white crystal and are produced by Polymer Factory Sweden AB. The chemical structure of these polymers is presented in Figures 1 and 2. The HBP were stored in an airtight container to protect from air humidity at 4°C, just opened for the experiments.

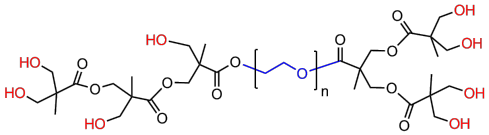

Figure 1: Idealized structure of G2 [25].

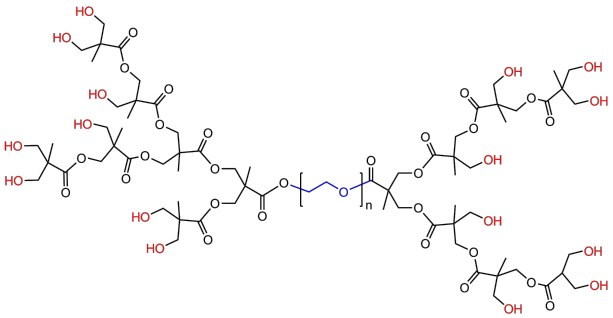

Figure 2: Idealized structure of G3 [25].

table

Table 1: Characteristics of the used polymers.

Sample	Molar mass M_W (g/mol)	Polydispersity M_W/M_n	Number of –OH per molecule
PEG 6000	5600-6600	–	2
PEG 8000	7000-9000	–	2
Dextran	35000-45000	–	–
PFLDHB-G2-PEG6k-OH	6696	1,42	8
PFLDHB-G3-PEG6k-OH	7625	1,3	16

In this work, lysozyme from hen egg white, EC 3.2.1.17, purchased from SIGMA-ALDRICH CHEMIE GmbH, Steinheim was used. The lysozyme has an average molar mass of 14600 g/mol and an activity of 120 000 U/mg. The lysozyme is a lyophilized powder and it was stored at 4°C. For the experiments, deionised water was used as solvent to prepare all the solutions.

2.2. Determination of the binodal curves

The cloud point method was selected to determine the binodal curve. Polymer aqueous solutions were prepared with a fixed compositions. The solution of one of the polymers was added drop-wise into a solution of a different polymer with a known mass, by using a syringe. The mixture was continuously stirred using a magnetic stirrer. After the addition of 3 ml, the mixture was observed to determine if it turned turbid in the following 1-2 minutes. Since it did not turn turbid, the last step was repeated until two phases formed, thus turning the mixture turbid. When the point on the binodal curve was obtained, observed by the turbidity of the mixture, the added weight was noted and 5 ml more were added. To obtain the second point of the binodal curve, deionized water was added by the same method until the mixture turned clear. The two steps were repeated in order to obtain points from all the binodal curve. The experiment was conducted at room temperature. The titration was performed for the systems PEG 6000 – Dextran – Water, PEG 8000 – Dextran – Water and G2 – Dextran – Water.

2.3. HPLC method

Size-exclusion, High-performance Liquid Chromatography (HPLC) system consisted of an auto sampler AS 4000, an interface D6000A, a pump L6200 from Hitachi/Merck, a column oven from Shimadzu, a refractive index detector K2301 from Herbert Knauer GmbH and one SUPREMA 100 A column was used. The mobile phase was Millipore water and the stationary phase was a polyhydroxymethacrylate copolymer network. Millipore water was also used as washing liquid for the auto sampler. No buffer was used.

The method was chosen considering that the peaks of the analysed polymers need to have retention times that ensure a good area of analysis. In the used column, the analysed polymers have bordering retention times, so to optimize the resolution the maximum column temperature, 80°C, was used. In Table 2, a summary of the method and measurement time is presented, and in Figure 3 the resultant chromatogram for each mixture.

Table 2: Summary of the methods and measurement times at 80°C.

	Flow (ml/min)	Time (min)
PEG 6000 – Dex	0,2	62
PEG 8000 – Dex	0,2	64
G2 – Dex	0,2	70
G3 – Dex	0,2	70

In Figure 3 it is possible to observe several peaks with retention times different from the peaks used to analyse the polymers of the mixture, which are a consequence of the polydispersity of the HBP and dextran. Most of these peaks can be ignored as they have very different retention times comparing to the main peaks, except the peak with a retention time of approximately 67 min (seen in (c) and (d) of Figure 3), which has some interference with the HBP peak. However, as it also appears on the calibration chromatograms without compromising the quality of the calibration curve, it was considered not to interfere with the measurement.

2.4. Calibration of the polymers

The calibration was performed for a concentration range of 0,01 to 0,2 wt% for PEG 6000, PEG 8000 and the HBP G2 and G3. For dextran the concentration range was of 0,01 to 0,3 wt%. In this step, Millipore water was used as diluter, eluent and washing liquid for the auto sampler. All the solutions were prepared at room temperature. The measurements were made in a balance scale with an accuracy of 0.0001 g. Bulk solutions were prepared for each polymer. The remaining solutions were prepared by diluting the bulk solutions with water. To determine the standard curves, the areas in the chromatography diagrams for each polymer with different concentrations were analysed with the use of OriginLab 9.0.

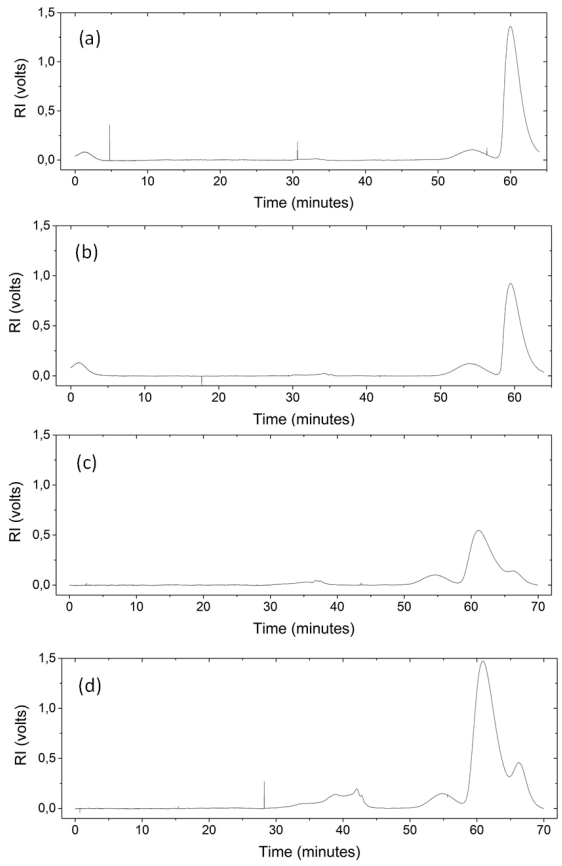

Figure 3: Chromatogram obtained from the studied aqueous solution at 80°C with a flow rate of 0,2 ml/min. (a) PEG 6000 – dextran 40 (b) PEG 8000 – dextran 40 (e) G2 – dextran 40 (d) G3 – dextran 40.

2.5. Determination of Tie Lines

Firstly, within the binodal curve, some ATPSs for each system were prepared. Then the prepared solutions were stirred with magnets stirring for 1-3 hours and put in a 25°C water bath for 72 hours to reach equilibrium – complete phase separation. After 72 hours, the two phases were separated with a syringe. Considering the limited interval of calibration, both the top and bottom phases were diluted with an appropriate amount of Millipore water. Thus, the concentration of each component in the two phases was measured with HPLC. To control the quality of the tie lines, the Lever Rule was applied. When the de-mixing point of the ATPS lies on the tie line, which was created by connecting two composition points for each phase, experiments were performed with acceptable accuracy.

2.6. Partitioning of the Lysozyme

Regarding the partitioning, two tie-lines were analysed for each type of system. The systems were prepared with two lysozyme concentrations, 0,3 and 1 wt %. The lysozyme absorbance was measured at 220 nm given that it was proven in this work that, at that wavelength, the linear polymers didn't influence the absorbance measurement for solution with a concentration lower than 1% of polymer. For the HBP, a calibration curve of the polymers was made in order to, knowing the polymer concentration, subtract the correspondent absorbance to the measured in the solution.

The systems were prepared and the lie lines were obtained with the same method as already mentioned. For the linear polymers, duplicates were made for each system.

To measure the lysozyme concentration in each phase, the solutions were diluted with Millipore water. A calibration was carried out with a concentration range of 0,001-0,01 wt % of lysozyme. The calibration solutions were prepared from two bulk solutions, a first one with 0,2 wt % of lysozyme and a second one with 0,1 wt %. The lysozyme was dissolved in water and the amount of both was weighted on a scale with accuracy of 0,0001 g. Other samples with lower concentration were diluted from the bulk solution by adding Millipore water. The two bulk solutions were prepared on different days, and the measurement of respecting diluted solutions also, confirming the applicability of the calibration.

A UVmini-1240 UV-Vis spectrophotometer from Shimadzu Corporation, a BRAND UV-Cuvette UV-Transparent Spectrophotometry were used to make all the spectrophotometric measurements. A NEW UV DATA MANAGER from Shimadzu Corporation was the used software to manage the data.

3. Model

3.1. Lattice Cluster Theory

Freed and co-workers [17, 18, 19, 20, 21] improved the FH theory by identifying and understanding its deficiencies, and calculating corrections. On the basis of de Gennes' work [26] treating long chain molecules as a self-avoiding walk on a lattice by the use of spins they developed the LCT for long chain molecules with different architectures. In this study, a LCT model applicable for a multicomponent polymer solution/blend, from Kulaguin and Zeiner [22] is used.

The LCT derives in the form of a cluster expansion in the inverse coordination number $1/z$ and the reduced interaction energy $\Delta\varepsilon_{ij}/k_BT$. Using Tables I-III [18] and the corrections given in [19], Equation (1) is defined for the Gibbs free energy contribution of the LCT, G_{LCT}, for an incompressible LCT with multi-components.

$$\frac{G_{LCT}}{N_L RT} = \sum_{i=1}^{n} \frac{\Phi_i}{M_i} \ln(\Phi_i) - \frac{\Delta S}{N_L RT} - \frac{\Delta E_1}{N_L RT} - \frac{\Delta E_2}{N_L RT} \quad (1)$$

The first term of Equation (1) emerges as the

contribution of the classical FH entropy, ΔS is the non-combinatorial correction term of the entropy, and ΔE_1 and ΔE_2 are the energy contributions of first and second order.

The correction term of the entropy and the energy contributions are calculated with the use of Equations 4, 10 and 17 of [22].

The calculated corrections are implemented in the model used, as the terms X_i^S, X_i^ε and $X_i^{\varepsilon^2}$, defined by Equations 5 to 9, 11 to 16 and 18 to 25 of [22], including a temperature-independent contribution to the χ parameter that arises from the corrections introduced by the chain connectivity and excludes volume constraints. In the X terms, two structural parameters, $b_{3,i}$ and $b_{4,i}$ – the number of branching points of three and four – are introduced in order to account for the chains' architecture. The use of this structural parameters assumes that there are at least two segments between two branching points, which for the used hyperbranched polymer this assumption is fulfilled. To consider the short chain branching the equations given in [27] have to be used. The advantage of the equations of this work is the simple way of describing the architecture and the reduced number of parameters.

In the framework of LCT, the interaction parameter $\Delta\varepsilon_{ij}$ is related to one contact point between segments. Hence, the product of coordination number and interaction energy describes the interaction of one segment. When the coordination number z tends to infinity ($z \to \infty$), $\frac{\Delta S}{N_L RT}$, $\frac{\Delta E_1}{N_L RT}$ and $\frac{\Delta E_2}{N_L RT}$ tend to zero, *i.e.*, the entropic LCT-contribution is reduced to the classical FH entropy and, in case the interaction energy also tends to zero ($\Delta\varepsilon_{ij} \to 0$), the energy contributions are reduced to the FH $\chi-$parameter.

3.2. Wertheim theory

In the systems to be studied in this work it is important to describe the molecules' association, as the Dextran T40 molecules have 3 OH-groups per glucose unit and the PEG/HB has the association sites on the oxygen.

Wertheim [23, 24] developed one theory that treats the associative bonds as directional forces between two association sites. This theory takes into account self and cross associations, *i.e.*, between molecules of the same type and different types. The Wertheim theory was transferred on a fully occupied lattice, so an incompressible fluid is regarded. As a result of the application of the Wertheim theory, the Gibbs energy has the extra addition (2)[28].

$$\frac{G_{asso}}{N_L RT} = \sum_i \Phi_i \left[\sum_{A_i} \left[\ln\left(X_{A_i}\right) - \frac{X_{A_i}}{2} \right] + \frac{1}{2} N_i^{asso} \right] \tag{2}$$

Where N_i^{asso} is the number of association sites per segments of component i, and X_{A_i} are the non-bonded segment fractions.

To apply this theory it is necessary to identify every associative site in the studied molecules [23, 24], which are divided by class according to the type of group that is responsible for the association, such as OH, amine or carbonyl. The non-bonded segment fractions can be calculated with Equation (3) [29][28]

$$X_{A_i} = \left[1 + \sum_j \sum_{B_j} \Phi_j X_{B_j} \Delta_{ij} \right]^{-1} \tag{3}$$

The cross association strength between two molecules Δ_{ij} is defined as:

$$\Delta_{ij} = K_{ij}^{asso} \left[\exp\left(\frac{\varepsilon_{ij}^{asso}}{k_B T} \right) - 1 \right] \tag{4}$$

where K_{ij}^{asso} is the association volume and ε_{ij}^{asso} is the association energy between two segments of two different components. These cross association parameters are calculated based on the self association ones, that must be fitted to experimental data:

$$K_{ij}^{asso} = \frac{K_{ii}^{asso} + K_{jj}^{asso}}{2} \tag{5}$$

$$\varepsilon_{ij}^{asso} = (1 - k_{ij}) \sqrt{\varepsilon_{ii}^{asso} \varepsilon_{jj}^{asso}} \tag{6}$$

where the parameter k_{ij} is introduced to consider the deviation of the association energy from the geometrical mixing rule, *i.e.*, the difference between $\sqrt{\varepsilon_{ii}^{asso} \varepsilon_{jj}^{asso}}$ and ε_{ij}^{asso}; K_{ii}^{asso} or K_{jj}^{asso}, and ε_{ii}^{asso} or ε_{jj}^{asso} are the association volumes and the association energies of one single component, respectively.

Finally, the total Gibbs free energy of the systems, when accounting for the architecture and the association interaction, is defined as:

$$\frac{G_{mix}}{N_L RT} = \frac{G_{asso}}{N_L RT} + \frac{G_{LCT}}{N_L RT} \tag{7}$$

4. Results

The Liquid-Liquid Equilibrium (LLE) was calculated with the Programming Software Free Pascal V2.6.4. The LCT+Wertheim model, which has been introduced in the theoretical part, has already been implemented to the program by Laboratory of Fluid Separations, TU Dortmund. Therefore, no programming work is required any more. The only work that needs to be done is calculating with this already existing program.

4.1. Liquid-liquid equilibria for the lysozyme-water system

The parameters describing the LLE of the binary subsystem lysozyme-water were be adjusted to experimental data, Figure 4. This step facilitates

the parameter adjustment in the quaternary system, where the partitioning of the lysozyme is calculated. For the modelling of the LLE of lysozyme solution, a linear structure will be considered and the 3D configuration will not be taken into account. The number of segments was defined based on the amino acids of the protein, so it equals 147, and the branching parameters are zero. The binary interaction, association and LCT parameters were fitted to the experimental results, and are presented in Table 3.

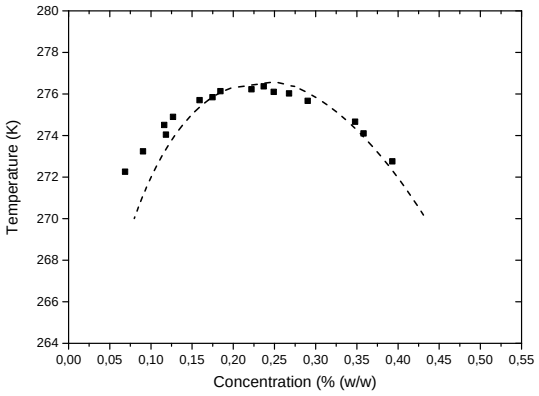

Figure 4: Liquid-liquid equilibrium of aqueous lysozyme solution. Symbols are experimental data [■]; The broken line is the model. Experimental data taken from Taratuta *et al* [30], from solutions in phosphate buffer with a pH of 7.

Table 3: Binary interaction, association and LCT parameters for the aqueous lysozyme solution.

Binary interaction energy ($\frac{\Delta\varepsilon_{ij}}{k_B}$) [K]	-25
Association energy ($\frac{\varepsilon_{ij}^{asso}}{k_B}$) [K]	559
Association parameter (K_{ij}^{asso})	0,1
Deviation of the geometrical mixing rule (k_{ij})	0,1

4.2. Liquid-liquid equilibria for ternary systems

The systems with linear polymers (PEG 6000/Dextran 40 and PEG 8000/Dextran 40) are calculated maintaining the LCT and Wertheim parameters coherent. The association parameters, association energy ($\frac{\varepsilon_{ii}^{asso}}{k_B}$) and association volume (K_{ii}^{asso}) of the pure solvent and the linear polymers were the first to be defined, based on former articles [22]. In the calculations for the linear polymer systems, the structural parameters taken into account are the molar mass of each component, $M_M i$, and the corresponding number of segments, M_i. In this case, give the linear structure, the number of branching points of 3, $b_{3,i}$, and 4, $b_{4,i}$ is zero. For the PEG polymer the number of segments is calculated by setting the segment size as the molar mass of the solvent, in this case water, meaning that each segment has a molar mass of 18 g/mol, therefore, PEG 6000 has 333 segments and PEG 8000 has 444 segments. The dextran molecule has rings as part of its structure, which cannot be described by the LCT. Considering that the space occupied by the glucose rings cannot be disregarded, for each ring an extra segment is accounted for. Thus, the number of segments per glucose is set as 7 – the number of carbons plus one. The dextran occupies 1597 segments. The interaction parameters were adjusted to the experimental data, and are presented in Table 4.

Table 4: Interaction parameters of LCT+Wertheim for systems with linear polymers.

PEG 6000 - water	-5,4
PEG 8000 - water	-4,8
Dextran - water	-9,5
Dextran - PEG 6000	14,5
Dextran - PEG 8000	13,5

In addition to the molecular structure parameters, the coordination number z also needs to be fixed. It describes the number of neighbour segments or next segments in the liquid. Originally, the LCT was developed at z=6, as a cubic lattice [17]. In this work, the coordination is also considered as 6. The modelled ATPS and the correspondent experimental data are illustrated in Figures 5 and 6. Symbols are experimental data [■]; The broken lines are the measured tie lines; the full lines are the modelled tie lines and binodal curve.

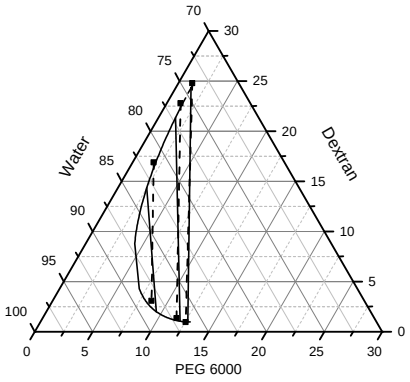

Figure 5: Experimental and LCT+Wertheim modelled points of ATPS consisting of linear polymers. ATPS consisting of PEG 6000 – dextran 40 – water.

The binodal curve can be described in good accordance with experimental data, but there are some deviations of the calculated tie lines and

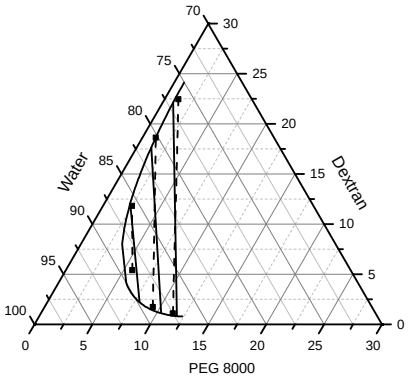

Figure 6: Experimental and LCT+Wertheim modelled points of ATPS consisting of linear polymers. ATPS consisting of PEG 8000 – dextran 40 – water.

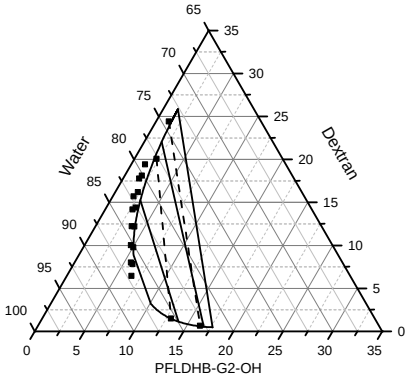

Figure 7: ATPS consisting of G2 – dextran 40 – water.

Table 5: Interaction parameters of LCT and Wertheim Association for the HBP.

G2-Dextran	20
G2-Water	-5
G3-Dextran	15
G3-Water	-6

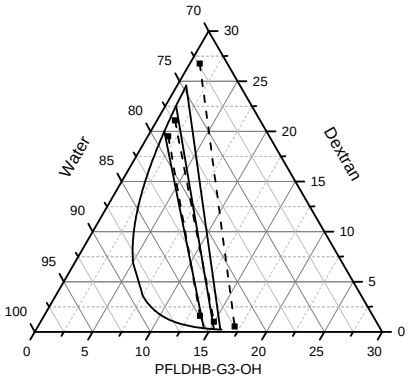

Figure 8: ATPS consisting of G3 – dextran 40 – water.

the experimental ones. The bigger deviations correspond to the tie-lines near the critical point, which are obtain with a bigger error experimentally, give that the equilibrium is more difficult to achieve. Although there are deviations in the tie lines, the agreement between experimental and modelling data is good for the linear system. Therefore, this LCT-Wertheim model can be applied to describe liquid-liquid equilibrium of PEG6000-Dextran-water and PEG8000-Dextran-water system, and it will be used to calculate the lysozyme partitioning in these systems.

The architecture of the HBPs will be determined by the chemical structure of the molecules, similar to former articles [22]. The HBPs are composed by a core of PEG its branching units are 2,2-bis(methylol)propionic acid (bis-MPA). The number of segments were defined considering that each bis-MPA molecule occupies 5 segments of the lattice, thus defining that each segment has a molar mass of 27. G2 occupies 248 segments and has one branching point of 3, and G3 occupies 346 lattice sites and has three branching points off 3. The interaction and association parameters where adjusted to the experimental data. The calculated and experimental values for both polymers are presented in Figures 7 and 8 and the used adjusted parameters can be found in Tables 5 and 6.

For the ATPS formed by G2 polymer, the binodal curve can be described in good accordance with experimental data, but there are big deviations between the calculated tie lines and the experimental ones. This can be explained by the chosen structural parameters, as these are the very influential parameters in the tie-line slope. Defining the bis-MPA monomer as occupying five segments in the lattice allows for good tie-line calculations for the G3 system, as can be seen in Figure 8, although this consideration did not apply for the G2 system. One reason for this could be the polydispersity of the HBP and the dextran. Consideration of dispersity can be an option to optimize the model. Similar systems, as PEG4000-dextran110, PEG10000-dextran40 and PEG10000-dextran110, can also be modelled with LCT and Wertheim theory [31]. Although deviations appear in some systems, this model can be accepted to describe the LLE of ATPS consisting of two polymers.

Additionally, a comparison can be made between the linear and the hyperbranched systems, PEG

Table 6: Association parameters of LCT and Wertheim Association for the HBP.

Association Energy		Association Volume	
G2	785	G2	0,0055
G3	779	G3	0,009
$k^{asso}_{G2-Water}$	0		
$k^{asso}_{G3-Water}$	0		
$k^{asso}_{G2-Dextran}$	0,085		
$k^{asso}_{G3-Dextran}$	0,045		

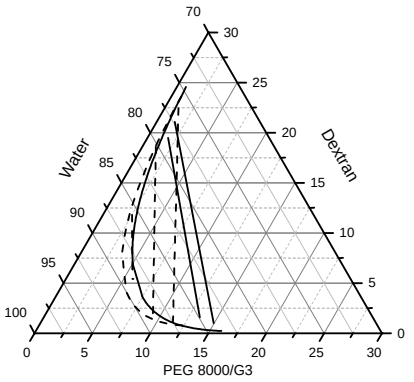

Figure 9: Experimental and LCT+Wertheim modelled points of ATPS consisting of G2 – Dextran – water and PEG 8000 – Dextran – water.

8000 system is compared with G3 in Figure 9. Comparing the ATPS based on the HBP and the ATPS including the PEG 6000 and 8000, it can be seen that the ATPS containing linear polymers has steeper tie lines. One disadvantage of the ATPS based on HBP is that the weight fraction of HBP polymer of the top (HBP-rich) phase is higher than in the ATPS containing linear polymers, which results in a higher requirement of HBP to form an ATPS. This fact is confirmed by the translation of the critical point in the ternary system to the right, meaning the minimum required amount of polymers to form an ATPS is larger for the systems containing HBP.

4.3. Partitioning

In the linear polymers based systems with 1% of lysozyme and in the HBP based a white deposit was detected in the interface, resulting of lysozyme precipitation. For the linear and HBP, the tie-lines show no deviation from the ones measured without lysozyme.

The partition coefficient of the lysozyme, K_P, was calculated with Equation (8) and the Tie Line Length (TLL) using Equation (9).

$$K_P = \frac{C_{i,BP}}{C_{i,TP}} \tag{8}$$

$$TLL = \sqrt{(C_{1,TP} - C_{1,BP})^2 + ... + (C_{n,TP} - C_{n,BP})^2} \tag{9}$$

Where $C_{i,TP}$ and $C_{i,BP}$ correspond to the equilibrium concentration of the protein in the top and bottom phases, respectively.

The obtained partition coefficients for ATPS with linear polymers as phase forming components are presented in Figure 10, with the correspondent deviations. It is possible to observe that for a lower protein concentration, 0,3 wt %, the partition coefficient increases with the TLL, but for a higher protein concentration, 1 wt %, the opposite occurs. In both cases, more partitioning is observed for an increasing TLL. Furthermore, the partitioning behaviour depends on the molar weight of the PEG used, since in the systems formed by PEG 6000 the lysozyme partitions to the bottom but in the case of PEG 8000 it partitions to the top.

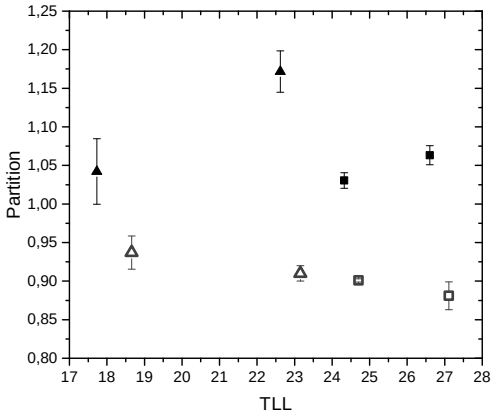

Figure 10: Partition coefficient experimentally obtained for ATPS formed by linear polymers PEG 6000 – Dextran (squares) and PEG 8000 – Dextran (triangles). The filled symbols correspond to systems with 0,3 wt % of lysozyme and the unfilled ones correspond to systems prepared with 1 wt % of lysozyme.

Considering the systems with 0,3 wt %, for a higher concentration of PEG, longer TLL, a larger amount of lysozyme partitions to the bottom phase, which can be explained by the solubility decrease in the PEG phase. Moreover, the systems with PEG 8000 show a higher partitioning behaviour for a given TLL. This may be related with the solubility of lysozyme in PEG solutions, since it decreases with PEG concentration e polymerization [32][33].

However, the measured concentrations for the systems with 1 wt % of lysozyme were unexpected, which can be related with the higher protein concentration, which may cause the precipitation of some of the protein in the interface of the systems.

Since the solubility in the PEG solution was verified in literature, a possible explanation may be a low solubility in the dextran phase. This would cause the protein to precipitate when in contact with that phase, lowering the partitioning coefficient. This effect would be more significant as the TLL increases, since then the dextran concentration increases as well. Furthermore, in Figure 10 it is possible to observe a tendency of the points with higher protein concentration, which suggests an independence from the PEG molar mass, and agrees with the given interpretation.

The interaction between the lysozyme and the phase forming polymers was modelled using a quaternary LCT model in combination with the Wertheim.For each system, PEG 6000 – dextran – water and PEG 8000 – dextran – water, the partition for one of the tie lines was adjusted. To test the model, the partitioning for the second tie line was calculated and compared to the measured value. In Figure 11 the results for a lysozyme concentration of 0,3 wt % are presented.

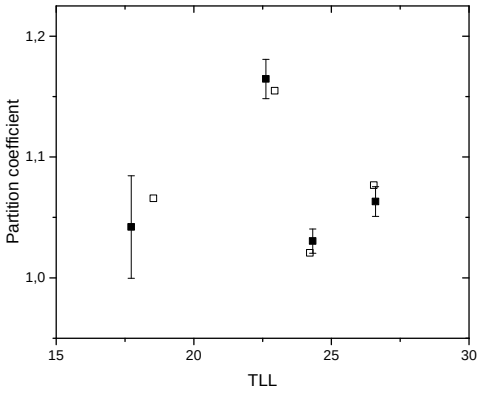

Figure 11: Partition coefficient experimentally obtained for ATPS formed by linear polymers PEG 6000 – Dextran – water and PEG 6000 – Dextran – water (filled symbols), and values calculated by the LCT+Wertheim (unfilled symbols), for a lysozyme concentration of 0,3 wt %.

Comparing the modelling results with the experimental data regarding the systems with 0,3 wt % of lysozyme, the model can be considered to describe the partitioning behaviour of the lysozyme in good accordance with the experimental data. Therefore, using the LCT+Wertheim model, the phase behaviour of quaternary systems can be described with an acceptable accuracy.

In Figure 12, the results for a lysozyme concentration of 1 wt % are presented. The calculated results do not fit the ones obtained experimentally, which can be explained by the already mentioned protein's precipitation. In order to test the model used for higher lysozyme concentrations, solubility measurements should be made for the conditions used in this work.

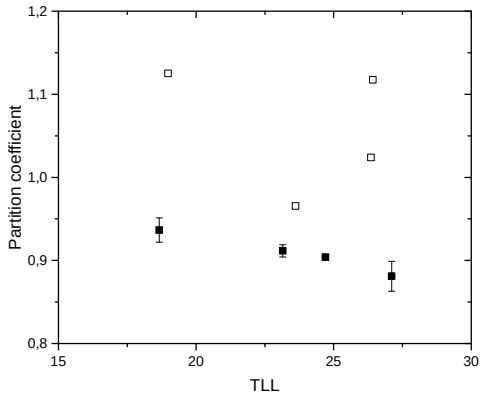

Figure 12: Partition coefficient experimentally obtained for ATPS formed by linear polymers PEG 6000 – Dextran – water and PEG 6000 – Dextran – water (filled symbols), and values calculated by the LCT+Wertheim (unfilled symbols), for a lysozyme concentration of 1 wt %.

Regarding the ATPS formed by HBP, a lot of precipitation was observed, and for that reason the obtained results were not modelled, since they do not represent the real behaviour of lysozyme in the ATPS based on G2 and G3. This problem could be solved by a test on the lysozyme solubility in solutions with G2 and G3 polymers.

5. Conclusions

Within this work, the phase behaviour of ATPS composed of linear polymer (PEG 6000/PEG 8000/dextran) was analysed, as well as the novel ATPS containing branched polymers (G2/G3). The LLE diagrams of the systems were determined by the investigation of the binodal curves and tie-lines. The partitioning behaviour of lysozyme in the PEG 6000 – dextran – water system and PEG 8000 – dextran – water systems was investigated. Additionally, the quaternary systems containing both lysozyme and HBP were also investigated. With all the experimental results of the LLE, a thermodynamic calculation model with Lattice Cluster Theory (LCT) combined with Wertheim theory was adjusted to describe the equilibrium of the systems with linear and branched polymers, as well as the partitioning of the lysozyme in the linear systems.

The obtained tie-lines have acceptable deviations to the demixing points. Reasons for these negligible deviations can be the non-complete phase separation and the non-optimized HPLC method. Comparing the experimental and modelled results

regarding the binodal curves for systems containing linear and branched polymers, it can be seen that the tie-lines of the systems containing branched polymers have steeper tie lines, which means that the minimum required amount of polymers to form the system is higher when using HBP. Additionally G2 and G3 polymers are more expensive than the used linear polymers. Therefore, in case the HBP based systems show an improvement on the partitioning of a product, an economic analysis would have to be made in order to understand if the improvement is worth the extra cost.

Modelling with LCT and Wertheim theory for binodal curves and tie lines can achieve a good accordance between experimental and calculated data for the systems containing linear polymers. In this case the association parameters are constant for both PEG 6000 and PEG 8000, and the structural parameters were calculated taking into account the molar mass of the polymers. The interaction parameters were adjusted for each polymer.

The modelling of the systems containing HBP was made by adjusting all the interaction and associative parameters related with the G2 and G3 polymers to the obtained experimental data. The structural parameters were defined by the polymers' structure. The binodal curve was well fitted in both systems, although the tie-lines for the G2 system showed some deviation to the experimentally obtained data. This can be explained by the polydispersity of the HBP, which is not considered in the model.

The lysozyme partitioning in systems containing linear polymers with a low protein concentration was also successfully modelled, using a quaternary LCT+Wertheim model. The interaction and association parameters between lysozyme and water were adjusted to literature data. The structural parameters were defined considering the biomolecule as a linear polymer with an amino acid per segment. The interaction and association parameters between the lysozyme and the polymers were determined by adjustment of the partitioning to the experimental data. The modelled partitioning behaviour was in good accordance with the experimental data.

It was not possible to measure the lysozyme concentration in the HBP based systems, because a part of the protein precipitated. In order to better study and compare the partitioning behaviour of biomolecules in ATPS containing HBP, solubility measurements should be made. The binodal curve and tie-lines were not influenced by the presence of lysozyme in any of the systems.

In further research, dispersity of the polymer can be considered in the model. This way, a higher accuracy could be achieved. Furthermore, as in the past [22], the model was successfully applied to calculate linear polymers based systems. Moreover in the present work it was also applied to HBP based systems. Therefore, it can be considered that the model has great potential to help with a more economically favourable development of novel ATPS.

References

[1] Florian M. Wurm. Production of recombinant protein therapeutics in cultivated mammalian cells. *Nature biotechnology*, 22(11):1393–1398, 2004.

[2] Ronald A. Rader. Fda biopharmaceutical product approvals and trends in 2012: Up from 2011, but innovation and impact are limited. *BioProcess International*, 11(3):18–27, 2013.

[3] AJJ Straathof. The proportion of downstream costs in fermentative production processes. *Comprehensive biotechnology*, 2:811–814, 2011.

[4] Uwe Gottschalk. Bioseparation in antibody manufacturing: the good, the bad and the ugly. *Biotechnology progress*, 24(3):496–503, 2008.

[5] Europen Medicines Agency. Guideline on setting specifications for related impurities in antibiotics. 2012.

[6] Thomas Reschke. *Modeling and design of aqueous two-phase systems*, volume 11 of *Schriftenreihe Thermodynamik*. Verl. Dr. Hut, München, 1. aufl. edition, 2014.

[7] Boris Y. Zaslavsky. *Aqueous two-phase partitioning: Physical chemistry and bioanalytical applications*. Dekker, New York, 1. print edition, 1995.

[8] Rosa, P A J, I. F. Ferreira, A. M. Azevedo, and M. R. Aires-Barros. Aqueous two-phase systems: A viable platform in the manufacturing of biopharmaceuticals. *Journal of chromatography. A*, 1217(16):2296–2305, 2010.

[9] Donald Othmer and Philip Tobias. Liquid-liquid extraction data- partial pressures of ternary liquid systems and the prediction of tie lines. *Industrial & Engineering Chemistry*, 34(6):696–700, 1942.

[10] Pedro González-Tello, Fernando Camacho, Gabriel Blázquez, and Francisco José Alarcón. Liquid−liquid equilibrium in the system poly(ethylene glycol) + mgso 4 + h 2 o at 298 k. *Journal of Chemical & Engineering Data*, 41(6):1333–1336, 1996.

[11] Edmond E, Ogston AG. An approach to the study of phase separation in ternary aqueous systems. *Biochemical Journal*, (109(4)):569–576, 1968.

[12] Edmond E, Ogston AG. Phase separation in an aqueous quaternary system. *Biochemical Journal*, (117):85–89, 1970.

[13] Erich A. Müller and Keith E. Gubbins. Molecular-based equations of state for associating fluids: A review of saft and related approaches. *Industrial & Engineering Chemistry Research*, 40(10):2193–2211, 2001.

[14] Andres Kulaguin Chicaroux and Tim Zeiner. Investigation of interfacial properties of aqueous two-phase systems by density gradient theory. *Fluid Phase Equilibria*, 2015.

[15] Paul J. Flory. *Principles of polymer chemistry*. Cornell Univ. Pr, Ithaca, 12. print edition, 1983.

[16] Maurice L. Huggins. Theory of solutions of high polymers 1. *Journal of the American Chemical Society*, 64(7):1712–1719, 1942.

[17] Jacek Dudowicz, Karl F. Freed, and William G. Madden. Role of molecular structure on the thermodynamic properties of melts, blends, and concentrated polymer solutions: comparison of monte carlo simulations with the cluster theory for the lattice model. *Macromolecules*, 23(22):4803–4819, 1990.

[18] Jacek Dudowicz and Karl F. Freed. Effect of monomer structure and compressibility on the properties of multicomponent polymer blends and solutions: 1. lattice cluster theory of compressible systems. *Macromolecules*, 24(18):5076–5095, 1991.

[19] Jacek Dudowicz, Karl F. Freed, and Jack F. Douglas. Modification of the phase stability of polymer blends by diblock copolymer additives. *Macromolecules*, 28(7):2276–2287, 1995.

[20] K. F. Freed, editor. *Phase Behaviour of Polymer Blends*. Advances in Polymer Science. Springer-Verlag, Berlin/Heidelberg, 2005.

[21] Karl F. Freed and Jacek Dudowicz. Influence of monomer molecular structure on the miscibility of polymer blends. In K. F. Freed, editor, *Phase Behaviour of Polymer Blends*, volume 183 of *Advances in Polymer Science*, pages 63–126. Springer-Verlag, Berlin/Heidelberg, 2005.

[22] Andres Kulaguin-Chicaroux and Tim Zeiner. Novel aqueous two-phase system based on a hyperbranched polymer. *Fluid Phase Equilibria*, 362:1–10, 2014.

[23] M. S. Wertheim. Fluids with highly directional attractive forces. i. statistical thermodynamics. *Journal of Statistical Physics*, (1-2):19–34, 1984.

[24] M. S. Wertheim. Fluids with highly directional attractive forces. ii. thermodynamic perturbation theory and integral equations. *Journal of Statistical Physics*, 35(1-2):35–47, 1984.

[25] Online catalog of hyperbranched peg products offered by polymer factory, July 2015.

[26] Shahin Khosharay, Mostafa Abolala, and Farshad Varaminian. Modeling the surface tension and surface properties of (co 2+ h 2 o) and (h 2 s+ h 2 o) with gradient theory in combination with spc–saft eos and a new proposed influence parameter. *Journal of Molecular Liquids*, 198:292–298, 2014.

[27] K. Langenbach and S. Enders. Development of an eos based on lattice cluster theory for pure components. *Fluid Phase Equilibria*, 331:58–79, 2012.

[28] Sabine Enders, Kai Langenbach, Philipp Schrader, and Tim Zeiner. Phase diagrams for systems containing hyperbranched polymers. *Polymers*, 4(1):72–115, 2012.

[29] K. Langenbach and S. Enders. Development of an {EOS} based on lattice cluster theory for pure components. *Fluid Phase Equilibria*, 331:58 – 79, 2012.

[30] Victor G. Taratuta, Andreas Holschbach, George M. Thurston, Daniel Blankschtein, and George B. Benedek. Liquid-liquid phase separation of aqueous lysozyme solutions: effects of ph and salt identity. *The Journal of Physical Chemistry*, 94(5):2140–2144, 1990.

[31] Andres Kulaguin Chicaroux and Tim Zeiner. Investigation of interfacial properties of aqueous two-phase systems by density gradient theory. *Fluid Phase Equilibria*, 2015.

[32] Ufuk Gündüz. Partitioning of bovine serum albumin in an aqueous two-phase system: optimization of partition coefficient. *Journal of Chromatography B: Biomedical Sciences and Applications*, 743(1):259–262, 2000.

[33] Matjaž Bončina, Jurij Reščič, and Vojko Vlachy. Solubility of lysozyme in polyethylene glycol-electrolyte mixtures: the depletion interaction and ion-specific effects. *Biophysical journal*, 95(3):1285–1294, 2008.